East European Journal of Physics. 4. 262-273 (2024)
DOI:10.26565/2312-4334-2024-4-27 ISSN 2312-4334

EXPLORING THE ELASTIC, MAGNETIC, THERMODYNAMIC AND ELECTRONIC PROPERTIES OF XNNi3 (X: Cd,In)CUBIC ANTI-PEROVSKITES

Jounayd Bentounes[a], Amal Abbad[b], Wissam Benstaali[b,*], Kheira Bahnes[b], Noureddine Saidi[b]
[a]*Faculty of Exact Sciences and Computer Sciences, Abdelhamid Ibn Badis University, Mostaganem (27000) Algeria*
[b]*Laboratory of Technology and Solids Properties, Faculty of Sciences and Technology, BP227, Abdelhamid Ibn Badis University, Mostaganem (27000) Algeria*
**Corresponding Author e-mail: ben_wissam@yahoo.fr*
Received July 12, 2024; revised September 18, 2024; accepted September 30, 2024

Density functional theory is used to investigate the structural, electronic, thermodynamic and magnetic properties of the cubic anti-perovskites $InNNi_3$ and $CdNNi_3$. Elastic and electronic properties were determined using generalized gradient approximation (GGA) and local spin density approximation (LSDA) approaches. The quasi-harmonic Debye model, using a set of total energy versus volume calculations is applied to study the thermal and vibrational effects. The results show that the two compounds are strong ductile and satisfy the Born-Huang criteria, so they are mechanically stable at normal conditions. Electronic properties show that the two compounds studied are metallic and non-magnetic. The thermal effect on the bulk modulus, heat capacity, thermal expansion and Debye temperature was predicted.
Keywords: *Anti-Perovskites; Electronic band structure; Elastic constants; First-principles calculations; Thermodynamic properties*
PACS: 61.50.Ah; 71.20.Nr; 62.20.Dc; 71.15.Mb; 65.40.Ba

1. INTRODUCTION

In recent years, the anti-perovskite carbides, nitrides and borides compounds have gained considerable attention because they have an extensive range of interesting physical and chemical properties. Their attractive physical properties derived from the association of magnetic phase transition and crystal lattice, such as nearly zero temperature coefficient of resistivity, magnetostriction, negative thermal expansion, giant magnetoresistance (GMR), and superconductivity at high temperature [1-7].

The ternary nitrides or carbides have the cubic anti-perovskite structure of the general formula XAM3(X are elements of (III–V) group, A is carbon or nitrogen, and M are transition metals) [8]. The cubic anti-perovskite type is an ordinary cubic perovskite where the metal atoms have exchanged positions with the non-metal atoms within the unit cell. The M metal atoms are positioned at the face-centered positions, the X metal atoms are positioned at the cube corner sites, and the non-metal atoms are positioned at the body-centered positions [9]. Because of the exceptional properties of several binary nitrides, ternary and higher nitrides have gained much attention during the last years, also, theoretical investigations of the physical properties of the anti-perovskite nitrides with alkali-earth metals have involved many interest [10–23]. Compared to the other member of these large family, the physical properties of the Ni-based cubic anti-perovskite compounds with a general composition MNNi3 (M = Cd and In) are less investigated. A more complete understanding of the physical properties of $CdNNi_3$ and InNNi3 is needed to ultimate technological applications of these compounds.

First-principles calculations offer one of the greatest tools for carrying out theoretical studies of significant number of physical and chemical properties of many materials with big accuracy. Nowadays it is possible to make clear and calculate properties of many solids which were in the past difficult to get with experiments.

Motivated by the above mentioned reasons and considering the lack of high order elastic constants for most anti-perovskite materials, we report in this paper a systematic study of the structural, elastic, thermodynamic and electronic properties for the two cubic anti-perovskite compounds $InNNi_3$ and $CdNNi_3$ using the full-potential linearized augmented plane wave (FPLAPW) method based on the density functional theory (DFT) within the generalized-gradient approximation (GGA) and the local spin density approximation (LSDA) approximations. The objective of the present paper is to theoretically predict and give a wide comprehension of the elastic, electronic and thermodynamic properties of the two compounds.

2. CALCULATION

In the present work Kohn–Sham equations [24] are solved to calculate the structural, electronic and magnetic properties of the cubic anti-perovskite $CdNNi_3$ and $InNNi_3$using the WIEN2K code [25, 26]. It is based on the full-potential linearized augmented plane wave method (FPLAPW) [27]. The two anti-perovskites are assumed to have an ideal cubic structure (space group is Pm3m (221) [28]). Basis functions were expanded as combinations of spherical harmonic functions inside non-overlapping spheres around the atomic sites (MT spheres) and in Fourier series in the interstitial region. The valence wave functions, inside the spheres are expanded up to l_{max}=10, the calculation gives

Cite as: J. Bentounes, A. Abbad, W. Benstaali, K. Bahnes, N. Saidi, East Eur. J. Phys. 4, 262 (2024), https://doi.org/10.26565/2312-4334-2024-4-27

84 K-points corresponding to a mesh (12×12×12) which is equivalent to 2000 K-points in the Brillouin zone (BZ). The wave functions in the interstitial region were expanded in plane waves with a cutoff of $k_{max}=7/R_{MT}$ (where R_{MT} is the average radius of the MT spheres). The muffin-tin radius R_{MT} is based on two conditions: (i) no core charge leaks out of MT spheres and (ii) no overlapping is permitted between spheres. The muffin–tin radii of the cubic $CdNNi_3$ anti-perovskite are taken to be 2.43, 1.62, and 1.82 atomic units (a.u.) for Cd, N and Ni respectively. The muffin–tin radii of the cubic $InNNi_3$ anti-perovskite are taken to be 2.24, 1.6, and 1.8 atomic units (a.u.) for In, N and Ni respectively. The lattice constants and bulk modulus are calculated by fitting the total energy versus volume according to the Murnaghan's equation of state [29]. For the exchange correlation functional, we have used the GGA [30] as well as the local spin density approximation (LSDA) [31].

3. RESULTS AND DISCUSSIONS

3.1. Structural and Elastic properties

In order to calculate the ground-state properties of $InNNi_3$ and $CdNNi_33$ antiperovskites, we performed the structural optimization by minimizing the total energy with respect to the cell parameters and the atomic positions. The equilibrium lattice parameters of both of the compounds are obtained by performing structural optimization and the calculated energy volume data is fitted to Murnaghan's equation of state.

To determine the magnetic ground state, both spin-polarized (ferromagnetic Fig. 1 (a) and (b)) and spin-unpolarized (non-magnetic Fig.1 (c) and (d)) calculations are also performed, for the magnetic and non-magnetic states as a function of volume (see Table 1), which is clearly indicating that the non-magnetic state has the lower energy as compared to the magnetic state for the two compounds, and therefore, the non-magnetic state is more favorable.

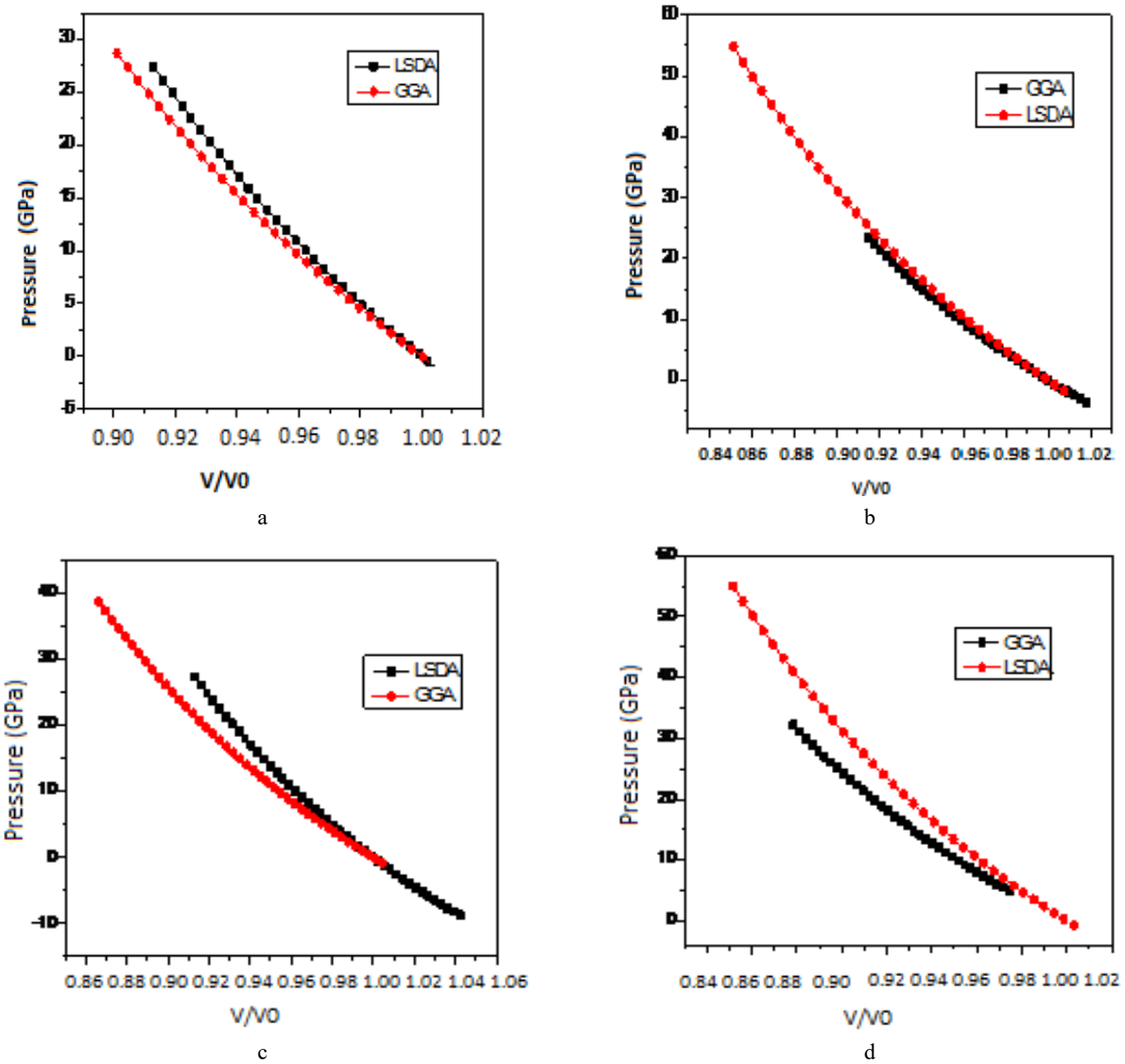

Figure 1. The variation of pressure (Gpa) as a function of v/v0 using LSDA and GGA approximations. (a) $CdNNi_3$ in ferromagnetic state. (b) $InNNi_3$ in ferromagnetic state. (a) $CdNNi_3$ in non-magnetic state. (a) $InNNi_3$ in non-magnetic state

Table 1. Calculated equilibrium lattice constant (a, in Å), bulk modulus (B, in GPa) and its pressure derivative (B_0), cell volumes (V, in $bhor^3$) and the minimum total energy (E, in Ry) in ferromagnetic (FM) and non-magnetic (NM) phases, for cubic anti-perovskites $CdNNi_3$ and $InNNi_3$ obtained with GGA and LSDA. Available experimental and theoretical results are quoted for comparison

Anti-perovskite	Parameters	LSDA	GGA	Exp	Other theoretical results
$CdNNi_3$	a [Å]	3.761(FM) 3.762 (NM)	3.807(FM) 3.857 (NM)	3.852[33]	-
	V	358.67(FM) 359.30 (NM)	372.369(FM) 387.4 (NM)	-	-
	B	234.49(FM) 235.85 (NM)	212.8(FM) 194.71 (NM)	-	-
	B_0	5.26(FM) 5.1 (NM)	5.26(FM) 5.1 (NM)	-	-
	E	-20401.22(FM) -20401.229 (NM)	-20422.36(FM) -20426.55 (NM)	-	-
$InNNi_3$	a [Å]	3.782(FM) 3.782 (NM)	3.826(FM) 3.879 (NM)	3.844[32] 3.862[33]	3.784(LDA) [34] 3.882(GGA)[34]
	V	365.119(FM) 365.142 (NM)	378.164(FM) 393.924 (NM)	-	-
	B	233.33(FM) 231.66 (NM)	210.81(FM) 176.77 (NM)	-	226.91(LDA) [34] 179.93(GGA)[34]
	B_0	4.758(FM) 4.6 (NM)	5.639(FM) 4.9 (NM)	-	4.761(LDA) [34] 4.281(GGA)[34]
	E	-20975.497(FM) -20975.499 (NM)	-20997.04(FM) -21001.12(NM)	-	-

The calculated bulk moduli B_0, the pressure derivatives of bulk modulus B' and the equilibrium lattice parameter a_0 using GGA and LSDA, are given in Table 01 with the available experimental and theoretical data for comparison [32-34]. Our calculated equilibrium lattice constant a_0 is in good agreement with the experimental data. We can see that, the use of the LSDA slightly underestimates the lattice constants comparing to GGA approximation which gives better theoretical results.

The elastic constants are elemental and very important for describing the mechanical properties of materials. They have significant information which can be obtained from ground state total energy calculations [35, 36]. The elastic constants are connected to a number of fundamental properties such as equation of state, interatomic potential, specific heat, phonon spectra, Debye temperature and melting point. They also provide information about the mechanical, dynamical behavior and the nature of forces operating in solids. The study of elasticity defines the properties of material that undergoes stress, deforms, and then recovers and returns to its original shape after stress stops.

To study the stability of cubic $CdNNi_3$ and $InNNi_3$ anti-perovskites, we have calculated the elastic constants at equilibrium lattice parameter within GGA and LSDA approaches, we have used the numerical first-principle calculation by computing the components of the stress tensor δ for small stains, by means of the method developed by Charpin and integrated in WIEN2K code which has been applied successfully in previous works [37–39]. In the case of cubic system, there are three independent elastic constants, namely C_{11}, C_{12}, and C_{44} to totally characterize the mechanical properties, the mechanical stability criteria for a cubic crystal are, its three independent elastic constants should satisfy the following relations given by Born and Huang [40]; $(C_{11}-C_{12})> 0$, $C_{12}> 0$, $C_{44}> 0$ and $C_{11}+C_{12}> 0$

The bulk modulus B is calculated using the following formula;

$$B = \frac{(C_{11}-2C_{12})}{3} \tag{1}$$

After that, the most important mechanical parameters for cubic anti-perovskites, namely shear modulus G, Young's modulus E, Poisson's ratio σ and Lamé's coefficients μ and λ, the anisotropy factor A, which are the main elastic moduli for applications, are calculated from the elastic constants of the single crystals using the following relations:

$$G = \frac{C11-C12+3C44}{5}, \tag{2}$$

$$E = \frac{9BG}{3B+G}, \tag{3}$$

$$\sigma = \frac{3B-E}{6B}, \tag{4}$$

$$\mu = \frac{E}{2(1+\sigma)}, \tag{5}$$

$$\lambda = \frac{\sigma E}{(1+\sigma)(1-\sigma)}, \quad (6)$$

$$A = \frac{2C44}{(C11-C12)}. \quad (7)$$

The computed values of the elastic constants for $CdNNi_3$ and $InNNi_3$ are given in Table 2. Till date, no experimental or theoretical data for $CdNNi_3$ are available to be compared with our computed results. We remark that C_{11}, C_{12} and C_{44} calculated using LSDA are higher than those calculated using GGA. Referring to Table 2, the values of B0 obtained from EOS fitting and elastic constants (B_0= (C_{11}+2C_{12})/3) are nearly same, which ensures that the computed elastic constants for $CdNNi_3$ and $InNNi_3$ are consistent. Moreover, this may be an approximation of the accuracy of our calculated elastic constants. Also from Table 2, we can compare our results against the Born-Huang criteria for stability, so our two compounds satisfy the Born-Huang criteria, so they are mechanically stable at normal conditions. The elastic constants for $InNNi_3$ are compared with theoretical study done by Z.F. Hou [34] and we can note that our results are in good agreement.

Table 2. Calculated elastic constants (C_{11}, C_{12}, C_{44} (GPa)), bulk modulus B_0 (GPa), Young's modulus E(GPa), Shear modulus G(GPa), Poisson's ratio σ, and Lamé's coefficients (λ and μ, in GPa) and anisotropy factor A for cubic anti-perovskites $CdNNi_3$ and $InNNi_3$ obtained with GGA and LSDA. Available theoretical results are quoted for comparison.

	$CdNNi_3$		$InNNi_3$	
	LSDA	GGA	LSDA	GGA
B_0	235.85[a],236.45[b]	190.47[a], 184.61[b]	231.66[a],232.8[b]	176.77[a],182.97[b]
C_{11}	399.42	258.60	412.60(356.77[c])	310.97(274.08[c])
C_{12}	157.47	147.62	142.89(164.23[c])	116.97(131.20[c])
C_{44}	84.94	41.49	61.72(69.06[c])	71.71(60.01[c])
G	97.89	46.61	84.89 (79.24[c])	80.61(64.35[c])
E	391.56	186.47	339.58(212.94[c])	322.44(172.37[c])
б	0.22	0.33	0.25(0.34[c])	0.20(0.33[c])
λ	194.50	244.61	225.49	136.60
μ	239.63	124.16	213.41	194.48
A	0.70	0.74	0.4577	0.74

[a]From Birch– Murnaghan's equation of state.
[b]FromB_0= (C_{11} +2C_{12})/3.
[c]From ref. [34]

The elastic anisotropy of crystals A has a significant interest in materials science in view of the fact that it is well correlated with the possibility to induce micro cracks in the materials. Isotropic crystal has an anisotropy factor equal to the unity, while any deviated value from 1 indicates anisotropy and this deviation is a measure of the degree of elastic anisotropy possessed by the crystal. The obtained values A are 0.45 for LSDA and 0.74 for GGA for $CdNNi_3$ and 0.36 for LSDA and 0.53 for GGA for $InNNi_3$, which are smaller than 1, which indicates a strong elastic anisotropy of the two compounds. The anisotropy is strong within LSDA compared to GGA, so the anisotropy factor is sensitive to the potential exchange.

Two other parameters are important for technological and engineering applications: Young's modulus E and Poisson's ratio σ. Young's modulus is defined as the ratio of tensile stress to tensile strain. It is frequently used to give a measure of rigidity of a solid, i.e., the larger is the value of Young's modulus, the rigid is the material. The calculated values for $CdNNi_3$ for LSDA and GGA are 391 and 186 respectively, so the material is stiffest using LSDA than GGA.

The value of Poisson's ratio σ is related with the volume change throughout uniaxial deformation. It presents information about the characteristics of the bonding forces. The σ = 0.25 and 0.5 are the lower and upper limit for the central forces in solids, respectively [41]. The values of Poisson's ratio σ obtained, suggest a considerable ionic contribution in intra-atomic bonding for these compounds.

The shear modulus G represents the resistance to reversible deformation, while the bulk modulus B gives the resistance to fracture. Pugh's index of ductility (B/G) allows us to know the ductile/brittle nature of a given material. The B/G critical value which separates ductile and brittle material is around 1.75 [42]. Our results show that the B/Gratio is 2.41 for LSDA and 3.91 for GGA for $CdNNi_3$ and 2.74 for LSDA and 2.26 for GGA for $InNNi_3$, which means that the two compounds are strong ductile.

The calculated density ρ, longitudinal, transverse and average sound velocity y_l, y_t and y_m and Debye temperature θ_D for the $InNNi_3$ and $CdNNi_3$ anti-perovskites using LSDA and GGA, are listed in Table 3. $CdNNi_3$ shows lower velocities and Debye temperature in the GGA scheme comparing to LSDA approximation.

Table 3. Calculated density ρ (in g/cm3), longitudinal, transverse and average sound velocity (V_l, V_t and V_m, respectively, in m/s) calculated from polycrystalline elastic moduli, and Debye temperature (θ_D in K), calculated from the average sound velocity, for $CdNNi_3$ and $InNNi_3$ anti-perovskites

		ρ	V_m	V_t	V_l	Θ_D
$CdNNi_3$	GGA	2.45	5059	4358	10028	255.62
	LSDA	2.66	7098.5	6055.3	11724	368.85
$InNNi_3$	GGA	2.42	6764.3	5761.5	10936	339.85
	LSDA	2.61	6653.9	5692.5	11492	342.87

3.2. Electronic properties

In order to explore the electronic properties of $CdNNi_3$ and $InNNi_3$ cubic anti-perovskites at equilibrium volume, spin-polarized calculations have been performed. We have studied the electronic properties of these two materials by the GGA and LSDA in order to compare between them. We have shown the electronic properties including band structure and density of states. The spin-polarized band structures of $CdNNi_3$ and $InNNi_3$ are plotted in Figs. 2 and 3, at the equilibrium lattice parameter for LSDA and GGA approximations. As can be seen, the two compounds studied are metallic. There is not much different from the DOSs using GGA or LSDA.

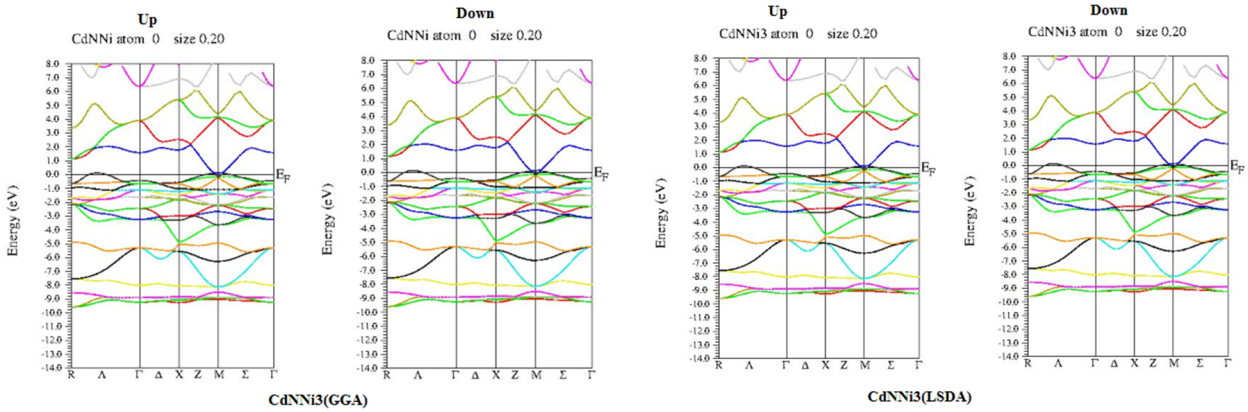

Figure 2. Spin-polarized band structures of $CdNNi_3$ using LSDA and GGA approximations

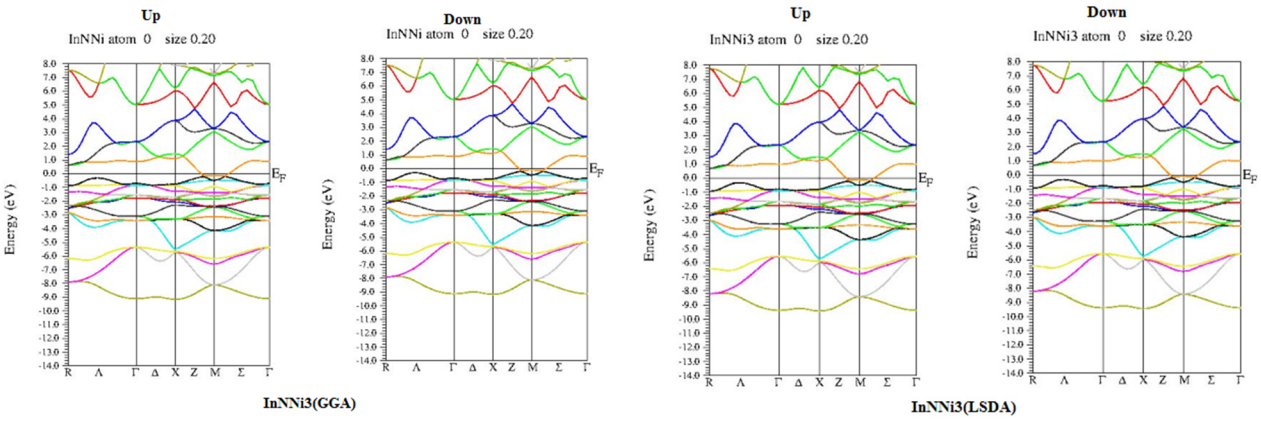

Figure 3. Spin-polarized band structures of $InNNi_3$using LSDA and GGA approximations

There is a total hybridization between the valence band and the conduction one; hence there is no band gap in the two materials. The nonexistence of the gap is a good indication of the presence of ionic bonding. This comes to confirm results obtained by elastic study.

The spin polarization total and partial density of states (DOS), using LSDA and GGA, are calculated and plotted in Figs. 4 and 5. The perfect symmetry of the states of spin "up" and the states of spin "down" is due to the fact that the Cd, In, N and Ni atoms are non-magnetic. For $CdNNi_3$ and for the two approaches LSDA and GGA, the bands between -9.5 eV and -8.5 eV are mainly due to the contribution of Cd 4d states, the second region between -8.1 eV and -5 eV is hybridization between N 2p and Ni 3d orbitals. The same contribution is observed in the region between -4.3 eV and 4 eV, and no contribution of Cd 4d states is seen in these two regions. This hybridization around Fermi level is responsible for the metallic behaviour observed in $CdNNi_3$. For $InNNi_3$, a different tendency can be noticed. The bandwidth in the lower part of the valence band (between -9 eV and -5.4 eV) is composed essentially from In 3d orbitals and N 2p states where the remaining part comes mostly from Ni 3d and some In 5p and N 2p states.

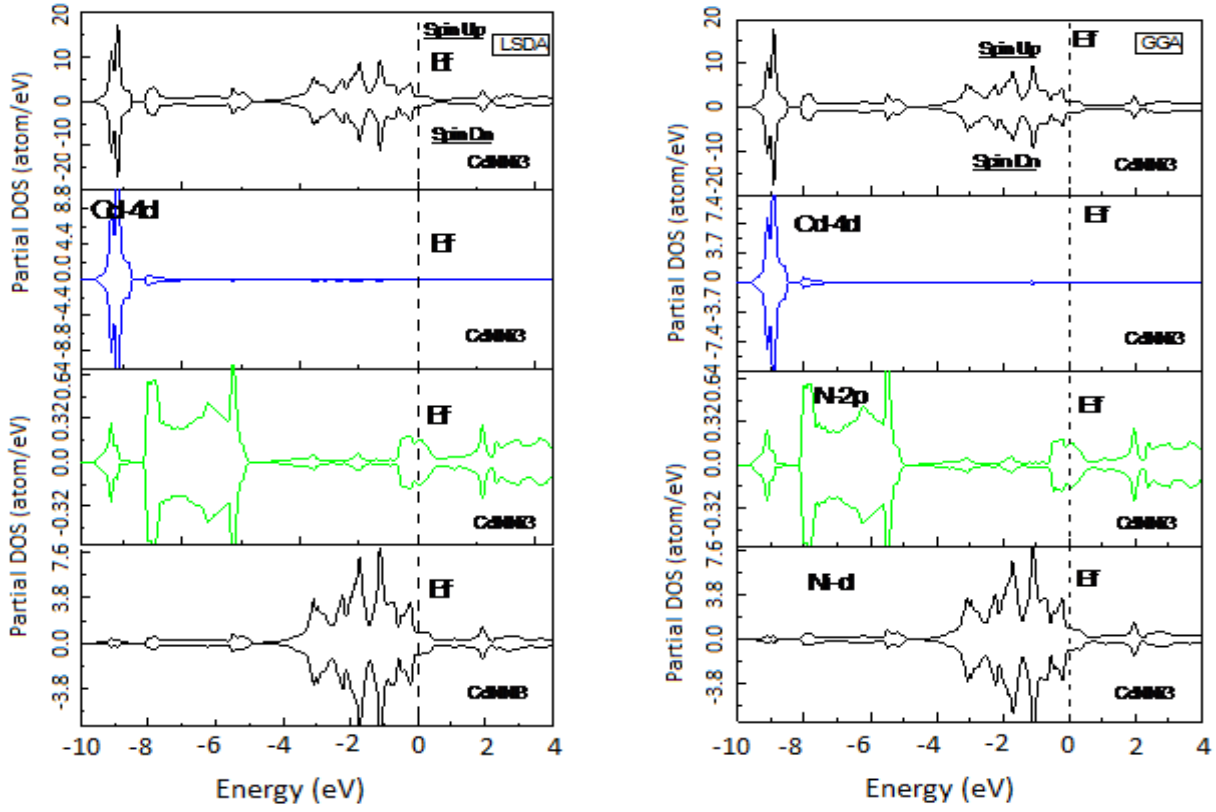

Figure 4. Total and partial density of States of $CdNNi_3$ anti-perovskite. (a) LSDA approximation. (b) GGA approximation. Fermi level is set to zero

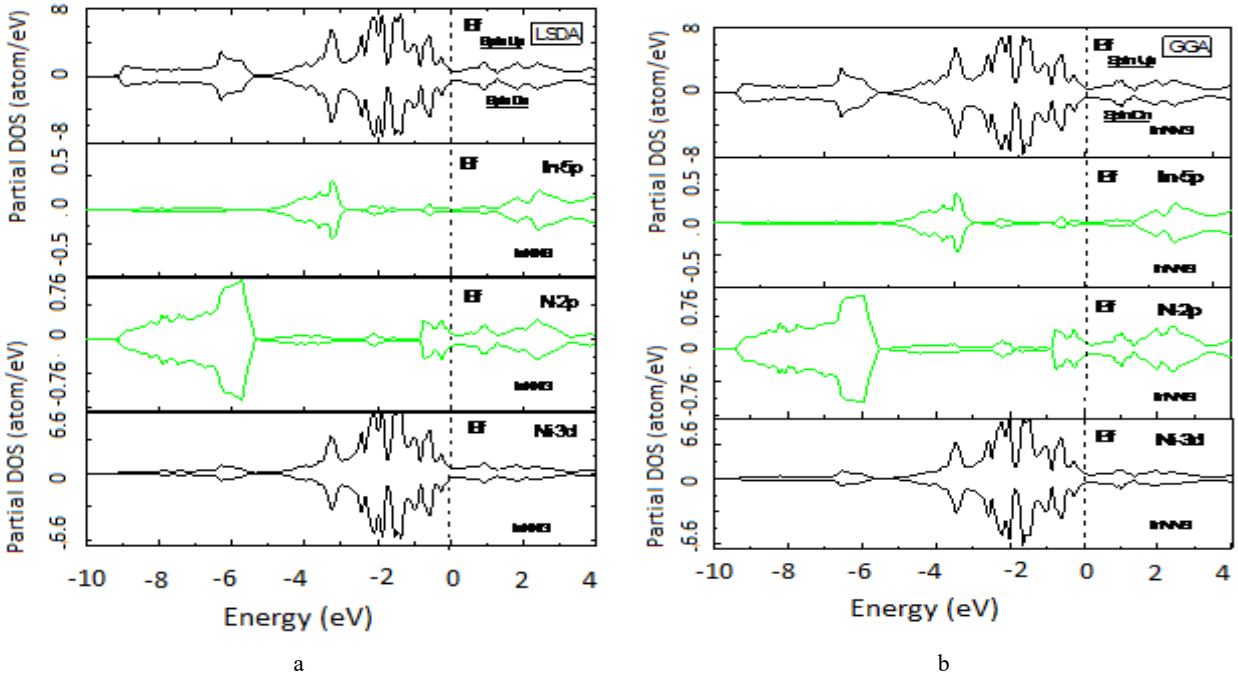

Figure 5. Total and partial density of States of $InNNi_3$ anti-perovskite. (a) LSDA approximation. (b) GGA approximation. Fermi level is set to zero

3.1 Thermodynamic properties

Exploration on the thermodynamic properties of solids is of great practical importance in engineering applications. In order to understand the thermodynamic properties of $CdNNi_3$ and $InNNi_3$ anti-perovskites under different temperatures and pressures, the quasi-harmonic Debye model as implemented in the Gibbs program [54] is applied.

The non-equilibrium Gibbs function $G^*(V, P, T)$ is giving by [43]:

$$G^*(V;P,T) = E(V) + PV + A_{vib}[\theta_D(V),T]. \quad (8)$$

Where *E(V)* is the total energy per unit cell of the crystal. *PV is* the constant hydrostatic pressure condition, θ_D *(V)* the Debye temperature and A_{vib} is the vibrational Helmholtz free energy, which can be written as [44, 45]:

$$A_{vib}(\theta_D,T) = nK_BT[\frac{9\theta_D}{8T} + 3\ln\left(1 - e^{\frac{-\theta_D}{T}}\circ - D\left(\frac{\theta_D}{T}\right)\right]. \quad (9)$$

Where *n* is the number of atoms per formula unit, KB is the Boltzmann's constant and $D\left(\frac{\theta_D}{T}\right)$ is the Debye integral. The Debye temperature θ_D for an isotropic solid is given as [45]:

$$\theta_D = \frac{\hbar}{\theta_D}\left[6\pi^2V^{\frac{1}{2}}n\right]^{\frac{1}{3}} f(\sigma)\sqrt{\frac{B_S}{M}}. \quad (10)$$

Where *M* is the molecular mass per unit cell and *BS* is the adiabatic bulk modulus, which is approximately given by the static compressibility;

$$B_S \cong B(V) = V\frac{d^2E(V)}{dV^2}. \quad (11)$$

$f(\sigma)$is given by Refs. [46, 47] and σ is the Poisson ratio. The non-equilibrium Gibbs function G^* can be minimized with respect to the volume *V* as:

$$\left[\frac{\partial G(V,P,T)}{\partial V}\right]_{P,T} = 0. \quad (12)$$

By solving equation (12) we obtain the thermal equation of state (EOS) *V (P, T)*. Thermodynamic quantities such as the heat capacities Cv (at constant volume), Cp (at constant pressure) and thermal expansion coefficient α*,* have been calculated by using the following relations [48];

$$C_V = 3nk\left[4D(\frac{\theta}{T}) - \frac{3\theta/T}{e^{\frac{\theta}{T}-1}}\right], \quad (13)$$

$$C_p = C_V(1 + \alpha\gamma T), \quad (14)$$

$$\alpha = \frac{\gamma C_V}{B_T V}. \quad (15)$$

B_T and γ are respectively the isothermal expansion coefficient and the Grüneisen parameter. Their formulas are given in reference [44].

Figures 6 (a) and (b) show the evolution of bulk modulus in terms of temperature of $CdNNi_3$ and $InNNi_3$ for different values of pressure using GGA approximation. From this figure, we can see that the bulk modulus decreases slowly at low temperature and then rapidly and linearly above 170 K linearly with increasing temperature at a given pressure. However, and at a given temperature, B increases with pressure. For T = 0K, B is minimal for 0 GPa and maximal for 30 GPa, it is evident that the impact of temperature and pressure on the bulk modulus of material are inverse. We can also notice that $CdNNi_3$ is hardest than $InNNi_3$. Also, in Figure 6 (c) and (d), we report the variation of bulk modulus versus pressure at different temperatures for the two compounds, we can see that B increase linearly with pressures.

In Figure 7 (a) and (b), we give the variation of the lattice constant a_0 as a function of temperatures for different pressures. We can notice that it stills constant until 170 K, after it increases linearly with temperature, however, a_0 decreases with increasing pressure (Fig. 7 (c) and (d). The tendencies are the same for the two compounds.

The thermal expansion coefficient α was calculated to reflect the temperature dependence of the volume. The calculated thermal expansion coefficient of $CdNNi_3$ and $InNNi_3$ as a function of temperature and pressure is shown in Fig. 8 (a) and (b). It is clear that the thermal expansion coefficient α rapidly increases with Tup to 500 K and then it gradually tends to a linear increase for higher temperatures, this means that the temperature dependence of α is very small at high temperature. The increase of α with T becomes smaller as pressure increases (Fig. 8 (c) and (d)). The thermal expansion coefficients of the two anti-perovskites exhibit similar tendency but it is larger for $InNNi_3$ comparing with $CdNNi_3$. In conclusion, we have found that the effects of T and P on α are opposite

The heat capacity Cv can be used to analyze vibrational properties of solids and can serve as a connection between microscopic structure and macroscopic thermodynamics property. Appropriately, the specific heat is the change in the internal energy per unit of temperature change. When we provide heat to a material, it will automatically cause an increase of temperature. This latter parameter provides us an insight into its vibrational properties' mandatory for many applications.

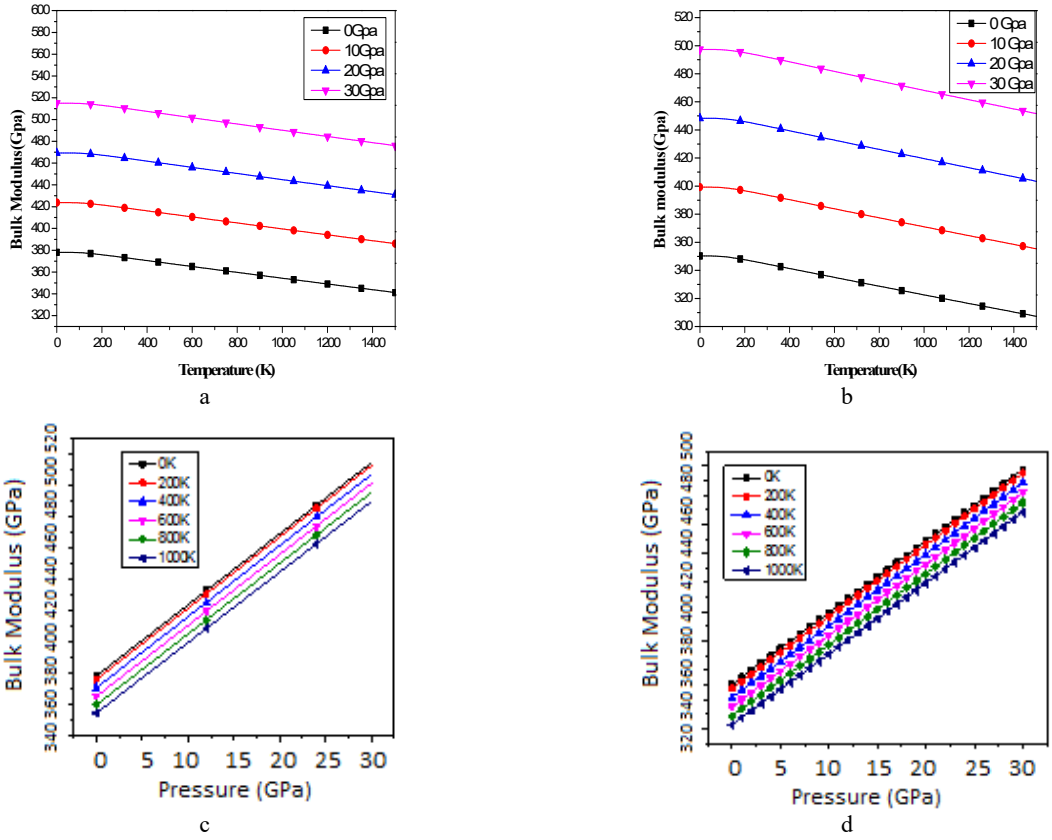

Figure 6. The variation of the bulk modulus. (a) As function of temperature at different pressures for $CdNNi_3$. (b) As function of temperature at different pressures for $InNNi_3$. (c) As function of pressure at different temperatures for $CdNNi_3$. (d) As function of pressure at different temperatures for $InNNi_3$

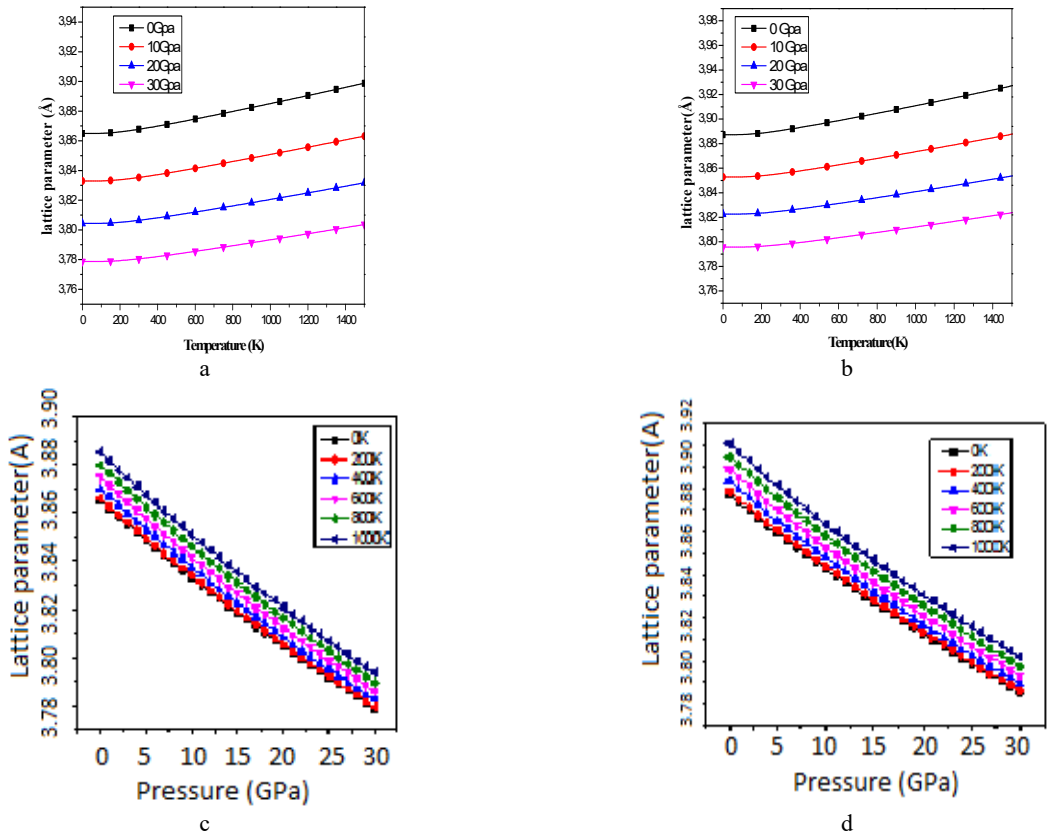

Figure 7. The variation of lattice parameter. (a) as function of temperature at different pressures for $CdNNi_3$. (b) as function of temperature at different pressures for $InNNi_3$. (c) as function of pressure at different temperatures for $CdNNi_3$. (d) as function of pressure at different temperatures for $InNNi_3$

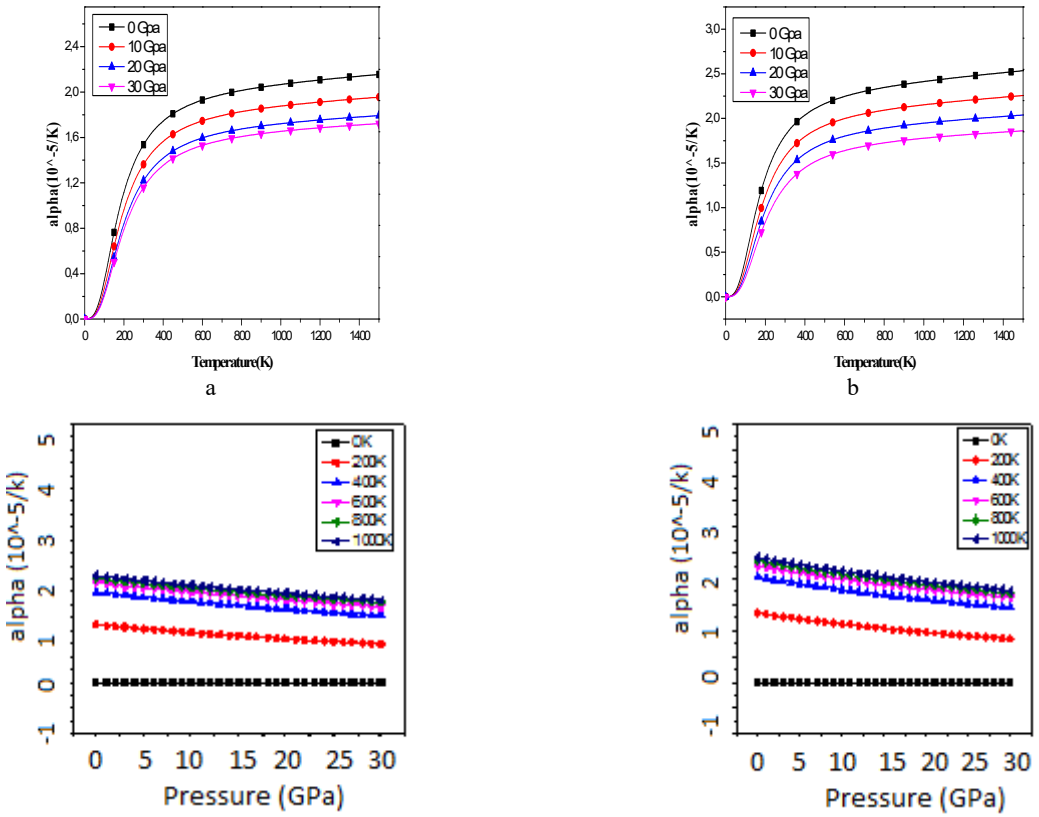

Figure 8. The variation of thermal expansion. (a) as function of temperature at different pressures for $CdNNi_3$. (b) as function of temperature at different pressures for $InNNi_3$. (c) as function of pressure at different temperatures for $CdNNi_3$. (d) as function of pressure at different temperatures for $InNNi_3$

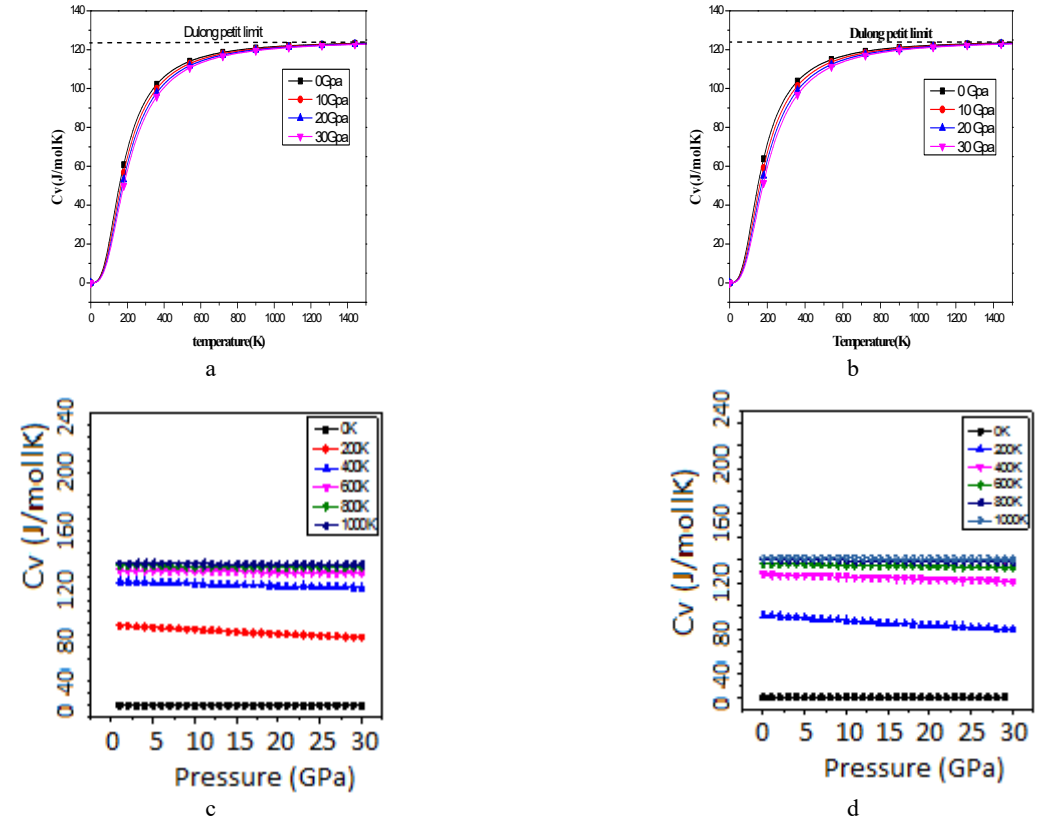

Figure 9. The variation of heat capacity. (a) as function of temperature at different pressures for $CdNNi_3$. (b) as function of temperature at different pressures for $InNNi_3$. (c) as function of pressure at different temperatures for $CdNNi_3$. (d) as function of pressure at different temperatures for $InNNi_3$

We present in Fig. 9 (a) and (b), the variation of the heat capacity C_V at constant volume versus temperature at 0, 10, 20 and 30 GPa. The variation of C_V for the investigated compound exhibits similar features for the two anti-perovskites. It can be seen that C_V shows a quick increase up to around 500 K, which is due to the anharmonic approximation. At higher temperature (>500 K), the anharmonic effect on Cv is suppressed, and Cv is close to the so-called Dulong-Petit limit [49] at high temperature, which is reasonable to all solids at high temperature, signifying that the thermal energy at high temperature excites all phonon modes. In addition, Fig. 08 indicates that the heat capacity is not affected by the variation of the pressure since the curves are superposed. The two compounds $CdNNi_3$ and $InNNi_3$ have similar values of heat capacity.

The Debye temperature θ_D is an important parameter since it determines the thermal characteristics of materials. A higher θ_D implies a higher thermal conductivity and melting temperature. Fig. 10 (a) and (b) display the dependence of the Debye temperature θ_D on temperature at several fixed pressures using GGA approach. $CdNNi_3$ has high Debye temperatures comparing to $InNNi_3$. θ_D is almost constant from 0 to 200 K and decreases linearly with increasing temperature especially. The Debye temperature increases with the enhancement of pressure. Our calculated θ_D is 739 K for $CdNNi_3$ and 710 K for $InNNi_3$ at T= 0 K and P= 0 GPa.

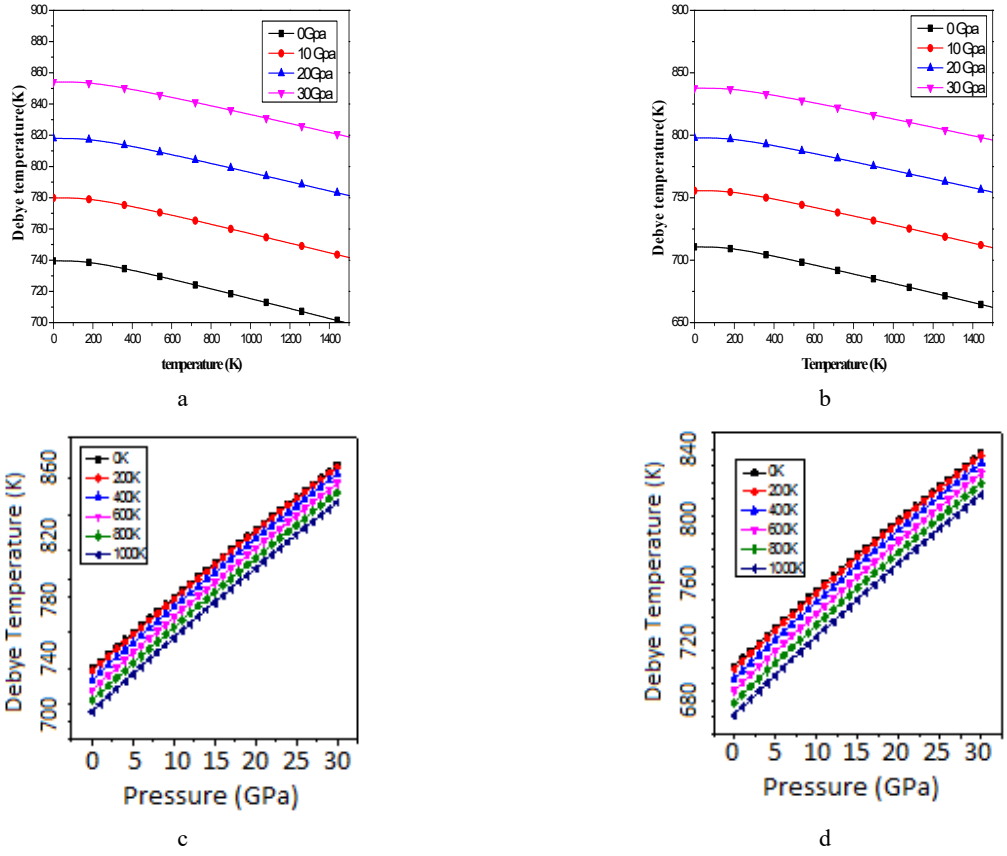

Figure 10. Variations of Debye temperature. (a) as function of temperature at different pressures for $CdNNi_3$. (b) as function of temperature at different pressures for $InNNi_3$. (c) as function of pressure at different temperatures for $CdNNi_3$. (d) as function of pressure at different temperatures for $InNNi_3$

3. CONCLUSIONS

In summary, we have performed first principles calculations based on the FPLAPW method within the GGA and LSDA to calculate the structural, electronic and thermodynamic properties of $CdNNi_3$ and $InNNi_3$ cubic anti-perovskites. The calculated equilibrium lattice constants of these compounds are in reasonable agreement with the available experimental data. We can see that our compounds are characterized by a high bulk modulus and show high stiffness, which make its very important for technological applications. In addition, the two compounds studied are metallic and non-magnetic which is in good agreement with experimental studies. Using the quasi-harmonic Debye model, we have obtained the pressure and temperature dependence of the bulk modulus, the heat capacity, Debye temperature, and thermal expansion coefficient of $CdNNi_3$ and $InNNi_3$. The two compounds $CdNNi_3$ and $InNNi_3$ have similar values of heat capacity and $CdNNi_3$ has high Debye temperatures comparing to $InNNi_3$.

ORCID

Jounayd Bentounes, https://orcid.org/0000-0003-2660-7102; **Amal Abbad,** https://orcid.org/0009-0006-1622-5564
Wissam Benstaali, https://orcid.org/0000-0003-4634-6210; **Kheira Bahnes,** https://orcid.org/0009-0007-3676-1126
Noureddine Saidi, https://orcid.org/0009-0004-5343-8572

REFERENCES

[1] C. Shang, X. Xiao, and Q. Xu", Coordination chemistry in modulating electronic structures of perovskite-type oxide nanocrystals for oxygen evolution catalysis," Coordination Chemistry Reviews, **485**, 215109(2023). https://doi.org/10.1016/j.ccr.2023.215109

[2] Z.-Y. Chen, N.-Y. Huang, and Q. Xu "Metal halide perovskite materials in photocatalysis: Design strategies and applications," Coordination Chemistry Reviews, **481**, 215031 (2023). https://doi.org/10.1016/j.ccr.2023.215031

[3] C. Ana, C. Dutra, and J.A. Dawson, "Computational Design of Antiperovskite Solid Electrolytes," J. Phys. Chem. C, **127**, 18256-18270(2023). https://doi.org/10.1021/acs.jpcc.3c04953

[4] X. Li, Y. Zhang, W. Kang, Z. Yan, Y. Shen, and J. Huo, "Anti-perovskite nitrides and oxides: Properties and preparation," Computational Materials Science, **225**, 112188 (2023). https://doi.org/10.1016/j.commatsci.2023.112188

[5] H.M.T. Farid, A. Mera, T.I. Al-Muhimeed, A.A. Al-Obaid, H. Albalawi, H.H. Hegazy, S.R. Ejaz, *et al*., "Optoelectronic and thermoelectric properties of A3AsN (A = Mg, Ca, Sr and Ba) in cubic and orthorhombic phase," Journal of Materials Research and Technology, **13**, 1495 (2021). https://doi.org/10.1016/j.jmrt.2021.05.032

[6] S.O. Volkova, S.P.S. Berdonosov, I.K. Shamova, B. Rahaman, A. Iqbal, T.S. Dasgupta, and A.N. Vasiliev, "Thermal and magnetic properties of $Cu_4O(SeO_3)_3$composed by ferrimagnetic O_2Cu_6units of edge-sharing OCu_4tetrahedra," Journal of Alloys and Compounds, **956**, 170346 (2023). https://doi.org/10.1016/j.jallcom.2023.170346

[7] M. Zhang, Z. Zhang, H. Cao, T. Zhang, H. Yu, J. Du, Y. Shen, *et al*., "Recent progress in inorganic tin perovskite solar cells," Mater. Today Energy, **23**, 100891 (2022). https://doi.org/10.1016/j.mtener.2021.100891

[8] J.B. Goodenough, W. Gräper, F. Holtzberg, D.L. Huber, R.A. Lefever, J.M. Longo, T.R. McGuire, and S. Methfessel, *Magnetic and other properties of oxides and related compounds*, Landolt–Bornstein, New Series, Group III, vol. 4a, (Springer, Berlin, 1970), pp. 126–275.

[9] K. Haddadi, A. Bouhemadoub, and L. Louail, "Ab initio investigation of the structural, elastic and electronic properties of the anti-perovskite $TlNCa_3$," Solid State Communications, **150**, 932 (2010).https://doi.org/10.1016/j.ssc.2010.02.024

[10] I.R. Shein, and A.L. Ivanovskii, "Electronic band structure and chemical bonding in the new antiperovskites $AsNMg_3$ and $SbNMg_3$", J. Solid State Chem. **177**, 61(2004). https://doi.org/10.1016/S0022-4596(03)00309-8

[11] M. Moakafi, R. Khenata, A. Bouhemadou, F. Semari, A. Reshak, and M. Rabah, "Elastic, Electronic and Optical Properties of Cubic Antiperovskites $SbNCa_3$ and $BiNCa_3$", Comput. Mater. Sci. **46**(4), 1051-1057 (2009). https://doi.org/10.1016/j.commatsci.2009.05.011

[12] A. Bouhemadou, R. Khenata, M. Chegaar, and S. Maabed, "First-principles calculations of structural, elastic, electronic and optical properties of the antiperovskite $AsNMg_3$," Phys. Lett. A, **371**, 337 (2007). https://doi.org/10.1016/j.physleta.2007.06.030

[13] C.M.I. Okoye, "First-principles optical calculations of $AsNMg_3$ and $SbNMg_3$," Mater. Sci. Eng. B,**130**, 101-107 (2006). https://doi.org/10.1016/j.mseb.2006.02.066

[14] F. Gabler, M. Kirchner, W. Schnelle, U. Schwarz, M. Schmitt, H. Rosner, R. Niewa, and Z. Anorg,"$(Sr_3N)E$ and $(Ba_3N)E$ (E = Sb, Bi): Synthesis, Crystal Structures, and Physical Properties," Allg. Chem. **630**, 2292 (2004).https://doi.org/10.1002/zaac.200400256

[15] D.A. Papaconstantopoulos, and W.E. Pickett, "Ternary nitrides BiNCa3 and PbNCa3: Unusual ionic bonding in the antiperovskite structure," Phys. Rev. B, **45**, 4008 (1992). https://doi.org/10.1103/PhysRevB.45.4008

[16] P.R. Vansant, P.E. Van Camp, V.E. Van Doren, and J.L. Martins, "Variable-cell-shape-based structural optimization applied to calcium nitrides", Phys. Rev. B, **57**, 7615 (1998). https://doi.org/10.1103/PhysRevB.57.7615

[17] P.R. Vansant, P.E. Van Camp, V.E. Van Doren, and J.L. Martins, "Electronic Structure and Pressure Dependence for Some Ternary Calcium Nitrides," Phys. Status Solidi (b), **198**, 87 (1996). https://doi.org/10.1002/pssb.2221980112

[18] P.R. Vansant, P.E. Van Camp, V.E. Van Doren, and J.L. Martins, "AsNCa3 at high pressure", Comput. Mater. Sci, **10**, 298 (1998).

[19] B.V. Beznosikov, "Predicted nitrides with an antiperovskite structure", J. Struct. Chem. **44**, 885-888 (2003). https://doi.org/10.1023/B:JORY.0000029831.93738.b1

[20] K. Haddadi, A. Bouhemadou, L. Louail, S. Maabed, and D. Maouche, "Structural and elastic properties under pressure effect of the cubic antiperovskite compounds ANCa 3(A = P, As, Sb, and Bi)," Phys. Lett. A, **373**, 1777-1781 (2009). https://doi.org/10.1016/j.physleta.2009.03.016

[21] K. Haddadi, A. Bouhemadou, L. Louail, and Y. Medkour, "Structural, elastic and electronic properties of XNCa3 (X = Ge, Sn and Pb) compounds," Solid State Commun. **149**, 619 (2009). https://doi.org/10.1016/j.ssc.2009.01.025

[22] I. Ahmad, S.J. Asadabadi, A. Bouhemadou, M. Bilal, R. Ahmad, "Electronic Properties of Antiperovskite Materials from State-of-the-Art Density Functional Theory," Journal of Chemistry, **2**, 1(2015). https://doi.org/10.1155/2015/495131

[23] K. Haddadi, A. Bouhemadou, L. Louail, F. Rahal, and S. Maabed, "Prediction study of the structural, elastic and electronic properties of ANSr3 (A= As, Sb and Bi)," Comput. Mater. Sci.46, 881-886 (2009). https://doi.org/10.1016/j.commatsci.2009.04.028

[24] W. Kohn, and L.S. Sham, "Self-Consistent Equations Including Exchange and Correlation Effects," Phys. Rev. A, **140**, 1133 (1965). https://doi.org/10.1103/PhysRev.140.A1133

[25] K. Schwarz, and P. Blaha, "Solid state calculations using WIEN2k", Computational Materials Science, **28**, 259-273 (2003). https://doi.org/10.1016/S0927-0256(03)00112-5

[26] P. Blaha, K. Schwarz, G.K.H. Madsen, D. Kvasnicka, and J. Luitz, *WIEN2K-An Augmented plane wave & Local Orbital Program for Calculating Crystal Properties*, (Techn. Universitat Wien, Austria, 2001).

[27] O.K. Andersen, "Linear methods in band theory," Phys. Rev. B, **12**, 3060 (1975). https://doi.org/10.1103/PhysRevB.12.3060

[28] C.J. Howard, B. J. Kennedy, and B.C. Chakoumakos, "Neutron powder diffraction study of rhombohedral rare-earth aluminates and the rhombohedral to cubic phase transition," Journal of Physics-Condensed Matter, **12**, 349 (2000). https://doi.org/10.1088/0953-8984/12/4/301

[29] F.D. Murnaghan, "The Compressibility of Media under Extreme Pressures," Proc. Natl. Acad. Sci. USA, **30**, 5390 (1944). https://www.ncbi.nlm.nih.gov/pmc/articles/PMC1078704/pdf/pnas01666-0028.pdf

[30] J.P. Perdew, A. Ruzsinszky, G.I. Csonka, O.A. Vydrov, G.E. Scuseria, L.A. Constantin, X. Zhou, and K. Burke, "Restoring the Density-Gradient Expansion for Exchange in Solids and Surfaces," Phys. Rev. Lett. **100**, 136406 (2008). https://doi.org/10.1103/PhysRevLett.100.136406
[31] U. Von Barth, and L. Hedin, "A local exchange-correlation potential for the spin polarized case," J. Phys C: Solid State Phys. **5**, 1629 (1972). https://doi.org/10.1088/0022-3719/5/13/012
[32] W.H. Cao, B. He, C.Z. Liao, L.H. Yang, L.M. Zeng, and C. Dong, "Preparation and properties of antiperovskite-type nitrides: $InNNi_3$ and InNCo3," J. Solid State Chem. **182**, 3353-3357 (2009). https://doi.org/10.1016/j.jssc.2009.10.002
[33] M. Uehara, A. Uehara, K. Kozawa, T. Yamazaki, and Y. Kimishima, "New antiperovskite superconductor ZnNNi3, and related compounds $CdNNi_3$ and $InNNi_3$," Physica C, **470**, 688 (2010). https://doi.org/10.1016/j.physc.2009.11.131
[34] Z.F. Hou, "Elastic properties and electronic structures of antiperovskite-type InNCo3 and $IInNNi_3$," Solid State Communications **150**, 1874-1879 (2010). https://doi.org/10.1016/j.ssc.2010.07.047
[35] V. Kanchana, G. Vaitheeswaran, A. Svane, and A. Delin, "First-principles study of elastic properties of CeO2, ThO2 and PoO2", J. Phys. Condens. Matter, **18**, 9615 (2006). https://doi.org/10.1088/0953-8984/18/42/008
[36] B. Ghebouli, M.A. Ghebouli, A. Bouhemadou, M. Fatmi, R. Khenata, D. Rached, T. Ouahrani, and S. Bin-Omran, "Theoretical prediction of the structural, elastic, electronic, optical and thermal properties of the cubic perovskites CsXF3 (X = Ca, Sr and Hg) under pressure effect," Solid State Sciences, **14**, 903-913 (2012). https://doi.org/10.1016/j.solidstatesciences.2012.04.019
[37] F. El Haj Hassan, and H. Akbarzadeh, "Ground state properties and structural phase transition of beryllium chalcogenides," Comput. Mater. Sci. **35**, 423 (2006). https://doi.org/10.1016/j.commatsci.2005.02.010
[38] R. Khenata, A. Bouhemadou, M. Sahnoun, Ali.H. Reshak, H. Baltache, and M. Rabah, "Elastic, electronic and optical properties of ZnS, ZnSe and ZnTe under pressure", Comput. Mater. Sci. **38**, 29 (2006). https://doi.org/10.1016/j.commatsci.2006.01.013
[39] A. Bouhemadou, R. Khenata, M. Kharoubi, T. Seddik, A.H. Reshak, and Y. Al-Douri, "FP-APW + lo calculations of the elastic properties in zinc-blende III-P compounds under pressure effects," Comput. Mater. Sci. **45**, 474 (2009). https://doi.org/10.1016/j.commatsci.2008.11.013
[40] M. Born, and K. Huang, *Dynamical Theory of Crystal Lattices*, (Clarendon, Oxford, 1956).
[41] J.P. Watt, and L. Peselnick, "Clarification of the Hashin-Shtrikman bounds on the effective elastic moduli of polycrystals with hexagonal, trigonal, and tetragonal symmetries," J. Appl. Phys. **51**, 1525(1980).
[42] S.F. Pugh, "Relations between the elastic moduli and the plastic properties of polycrystalline pure metals," Philos. Mag. **45**, 823-843 (1954). https://doi.org/10.1080/14786440808520496
[43] M.A. Blanco, E. Francisco, and V. Luaña, "GIBBS: isothermal-isobaric thermodynamics of solids from energy curves using a quasi-harmonic Debye model," Comput. Phys. Commun. **158**, 57 (2004). https://doi.org/10.1016/j.comphy.2003.12.001
[44] M.A. Blanco, A.M. Pendás, E. Francisco, J. M. Recio, and R. Franco, "Thermodynamical properties of solids from microscopic theory: applications to MgF_2 and Al_2O_3," J. Mol. Struct. Theochem. **368**, 245 (1996). https://doi.org/10.1016/S0166-1280(96)90571-0
[45] M. Flórez, J.M. Recio, E. Francisco, M.A. Blanco, and A.M. Pendás, "First-principles study of the rocksalt–cesium chloride relative phase stability in alkali halides,", Phys. Rev. B, **66**, 144112 (2002). https://doi.org/10.1103/PhysRevB.66.144112
[46] E. Francisco, J.M. Recio, M.A. Blanco, A. Martín Pendás, and A. Costalesm, "Quantum-Mechanical Study of Thermodynamic and Bonding Properties of MgF2," J. Phys. Chem. A, **102**, 1595-1601 (1998). https://doi.org/10.1021/jp972516j
[47] E. Francisco, M.A. Blanco, and G. Sanjurjo, "Atomistic simulation of SrF2 polymorphs," Phys. Rev. B, **63**, 094107 (2001). https://doi.org/10.1103/PhysRevB.63.094107
[48] R. Hill, "The Elastic Behaviour of a Crystalline Aggregate," Proc. Phys. Soc. London A, **65**, 349 (1952). https://doi.org/10.1088/0370-1298/65/5/307
[49] A.T. Petit, and P.L. Dulong, "Recherches de la Theorie de la Chaleur," Ann. Chim. Phys. **10**, 395 (1819).

ДОСЛІДЖЕННЯ ПРУЖНИХ, МАГНІТНИХ, ТЕРМОДИНАМІЧНИХ ТА ЕЛЕКТРОННИХ ВЛАСТИВОСТЕЙ КУБІЧНИХ АНТИПЕРОВСКІТІВ XNNi3 (X: Cd, In)

Жонаід Бентунес[a], Амал Аббад[b], Віссам Бенстаалі[b], Хейра Бахнес[b], Нуреддін Саїді[b]

[a]Факультет точних наук і комп'ютерних наук, Університет Абдельхаміда Ібн Бадіса, Мостаганем (27000), Алжир
[b]Лабораторія технології та властивостей твердих тіл, факультет природничих наук і технологій, BP227, Університет Абдельхаміда Ібн Бадіса, Мостаганем (27000), Алжир

Теорія функціонала густини використовується для дослідження структурних, електронних, термодинамічних і магнітних властивостей кубічних антиперовскітів $InNNi_3$ і $CdNNi_3$. Пружні та електронні властивості були визначені за допомогою підходів узагальненої градієнтної апроксимації (GGA) та локальної спінової апроксимації (LSDA). Для вивчення теплових і вібраційних ефектів використовується квазігармонічна модель Дебая з використанням набору розрахунків повної енергії та об'єму. Результати показують, що дві сполуки є міцними пластичними та задовольняють критерії Борна-Хуанга, тому вони механічно стабільні за нормальних умов. Електронні властивості показують, що дві досліджувані сполуки є металевими та немагнітними. Було передбачено тепловий вплив на об'ємний модуль, теплоємність, теплове розширення та температуру Дебая.

Ключові слова: *антиперовскіти; структура електронної смуги; пружні константи; розрахунки перших принципів; термодинамічні властивості*